Neoplasia • Vol. 3, No. 6, 2001, pp. 480–488

www.nature.com/neo

Imaging TCR-Dependent NFAT-Mediated T-Cell Activation with Positron Emission Tomography *In Vivo*[1]

Vladimir Ponomarev, Michael Doubrovin*, Clay Lyddane†, Tatiana Beresten*, Julius Balatoni‡, William Bornman§, Ronald Finn‡, Timothy Akhurst¶, Steven Larson¶, Ronald Blasberg*, Michel Sadelain† and Juri Gelovani Tjuvajev**

*Departments of Neurology and Radiology, †Immunology Program, Gene Transfer and Somatic Cell Engineering Facility, ‡Radiochemistry/Cyclotron Core Facility, §Preparative Synthesis Core Facility, ¶Nuclear Medicine Service, Memorial Sloan Kettering Cancer Center, New York, NY 10021

Abstract

A noninvasive method for molecular imaging of T-cell activity *in vivo* would be of considerable value. It would aid in understanding the role of specific genes and signal transduction pathways in the course of normal and pathologic immune responses, and could elucidate temporal dynamics and immune regulation at different stages of disease and following therapy. We developed and assessed a novel method for monitoring the T-cell receptor (TCR)-dependent nuclear factor of activated T cells (NFAT)-mediated activation of T cells by optical fluorescence imaging (OFI) and positron emission tomography (PET). The herpes simplex virus type 1 thymidine kinase/green fluorescent protein [*HSV1-tk/GFP* (*TKGFP*)] dual reporter gene was used to monitor NFAT-mediated transcriptional activation in human Jurkat cells. A recombinant retrovirus bearing the NFAT-TKGFP reporter system was constructed in which the *TKGFP* reporter gene was placed under control of an artificial *cis*-acting NFAT-specific enhancer. Transduced Jurkat cells were used to establish subcutaneous infiltrates in nude rats. We demonstrated that noninvasive OFI and nuclear imaging of T-cell activation is feasible using the NFAT-TKGFP reporter system. PET imaging with [^{124}I]FIAU using the NFAT-TKGFP reporter system is sufficiently sensitive to detect T-cell activation *in vivo*. PET images were confirmed by independent measurements of T-cell activation (e.g., CD69) and induction of GFP fluorescence. PET imaging of TCR-induced NFAT-dependent transcriptional activity may be useful in the assessment of T cell responses, T-cell–based adoptive therapies, vaccination strategies and immunosuppressive drugs. *Neoplasia* (2001) **3,** 480–488.

Keywords: molecular imaging, T-cell activation, herpes virus type 1 thymidine kinase, FIAU, PET.

Introduction

The analysis of molecular and biochemical events occurring *in vivo* during T-cell activation requires invasive tissue sampling. The recourse to invasive procedures often hinders and eventually precludes serial studies in the same subject, and does not provide spatial information concerning activated T-cell localization. By limiting studies to biopsy material, such investigations fail to provide a whole-body evaluation of developing immune responses. New technologies are needed to permit biochemical investigation *in situ* and repeatedly over time if necessary. Noninvasive whole-body imaging of T-cell activity would be of a considerable value; it would allow identification of sites and temporal dynamics of T-cell activation and provide a way to monitor trafficking of T cells during primary and memory responses. To visualize T-cell activation *in vivo*, we developed a T-cell receptor (TCR)-dependent, nuclear factor of activated T cells (NFAT)-sensitive TKGFP dual-reporter system that could be imaged using positron emission tomography (PET) [1–4] and whole-body optical fluorescence imaging (OFI) [5].

TCR interactions with MHC–peptide complexes expressed on antigen-presenting cells initiate T-cell activation, resulting in transcription mediated by several factors including NFAT. The TCR-specific NFAT family of transcription factors contains five distinct members. NFATs 1 to 4 share a highly conserved DNA binding domain and contribute to regulating a number of target genes, including interleukin 2 (IL-2) and other cytokines [6–9]. Their transcriptional activity is dependent on cytoplasmic dephosphorylation by the calcium-dependent serine phosphatase calcineurin and subsequent nuclear translocation, a process arrested by the calcineurin inhibitors Cyclosporin A and FK506 [6].

Abbreviations: HSV1-tk, herpes simplex virus type 1 thymidine kinase; GFP, green fluorescent protein; PET, positron emission tomography; FIAU, 2′-fluoro-2′-deoxy-1-β-D-arabinofuranosyl-5-iodo-uracil; FACS, fluorescence-activated cell sorting; DMEM, Dulbecco's modified Eagle medium; RPMI-1640, Roswell Park Memorial Institute series 1640 medium; OFI, optical fluorescence imaging; TCR, T-cell receptor; NFAT, nuclear factor of activated T cells; Luc, luciferase; PMA, phorbol 12-myristate 13-acetate; ELISA, enzyme-linked immunosorbent assay; CMV, cytomegalovirus; VSV-G, vesicular stomatitis virus G-protein; FCS, fetal calf serum; IL-2, interleukin 2

Address all correspondence to: Dr. Juri Gelovani Tjuvajev, Departments of Neurology and Radiology, Memorial Sloan Kettering Cancer Center, Room K923, 1275 York Avenue, New York, NY 10021. E-mail: gelovani@neuro1.mskcc.org

[1]This work was supported by NIH grants P50 CA86438-01, RO1 CA57599-01, RO1 CA76117-01, R24CA98023, PO1 CA-59350, and DOE grant FG03-86ER60407.
Received 31 August 2001; Accepted 20 September 2001.

In this paper, we describe the development of a recombinant self-inactivating retroviral vector encoding *TKGFP* and its use to monitor Jurkat T-cell activation by fluorescent microscopy, fluorescence-activated cell sorting (FACS) and radiotracer assays. We demonstrate that the same reporter system can be used to noninvasively monitor TCR-induced NFAT-mediated activation of subcutaneous Jurkat T-cell infiltrates *in vivo* by OFI and PET imaging.

Materials and Methods

Generation of Cis-NFAT/TKGFP and TKGFP Reporter Vectors

The *TKGFP* fusion gene and the SFG-TKGFP retroviral vector, which constitutively expresses *TKGFP*, were described previously [10]. To generate the *Cis*-NFAT/TKGFP vector, the *TKGFP* cDNA was cloned into the plasmid pNFAT-Luc (Stratagene, La Jolla, CA), replacing the luciferase gene. The *Bam*HI–*Not*I fragment containing the NFAT enhancer element, TATA-box, and *TKGFP* was then subcloned into the multicloning site of pLXSN (Clontech, Palo Alto, CA), 5′ to the neomycin phosphotransferase gene and the SV40 promoter. The *Nhe*I–*Nhe*I fragment containing the pBR322 backbone and most of the viral 3′LTR was replaced with pUC19 and a crippled 3′LTR (*Nhe*I–*Sac*I deletion) to generate dxNFATtgn. To potentiate NFAT-induced *TKGFP* expression, the adaptor containing the sequence of the minimal cytomegalovirus (CMV) promoter (from pBI-GL vector, Clontech) was introduced in the dxNFATtgn vector between the *Xba*I and *Eco*RI sites, replacing the original TATA-box, to create dcmNFATtgn. A negative control vector, termed dxRtgn, was constructed by replacing the NFAT responsive element with a random sequence of the same length. DNA (10 μg) was transfected into the GPG29 packaging cell line as previously described using the calcium phosphate method [11]. Vesicular stomatitis virus G-protein (VSV-G)–pseudotyped retroviral particles were used as cell-free viral stocks to transduce Jurkat cells.

Cell Lines

Jurkat cells bearing a functional TCR were kindly provided by Dr. P. King (Hospital for Special Surgery, Cornell University, NY) and grown in suspension in RPMI-1640 media supplemented with 10% fetal calf serum, L-glutamine, penicillin, and streptomycin (Invitrogen, Carlsbad, CA). The *in vitro* transduction of Jurkat cells with retroviral vectors was accomplished by exposing the cells to a filtered (0.45 μm) culture medium obtained from the vector producer cells for 24 hours in the presence of polybrene (8 μg/ml). Two days later, the media was supplemented with 1 mg/ml of G418 (Invitrogen) to select for transduced cells, and grown either as a bulk transduced culture or cloned by limiting dilution in 96-well plates. Clones were re-analyzed by FACS and clones with low basal levels of green fluorescent protein (GFP) fluorescence and high inducible levels after stimulation were selected.

Stimulation of Jurkat Cells In Vitro

Nonspecific stimulation transduced and wild-type Jurkat cells was performed with phorbol 12-myristate 13-acetate (PMA) 10 ng/ml and ionomycin 2.2 μm/l (Sigma, St. Louis, MO). TCR-specific stimulation of the cells was performed using plates precoated with anti–human CD3 antibody (1 μg/ml, Pharmingen, San Diego, CA) and soluble anti–human CD28 antibody (1 μg/ml, Pharmingen). A costimulation signal was provided with soluble anti–human CD28 antibody at a concentration of 1 μg/ml (Pharmingen). The specificity of the reporter system was assessed by blocking the activation of the NFAT transcription factor by adding 200 ng/ml of Cyclosporin A (Sigma) to the culture medium.

Flow Cytometry

Anti-human antibodies against CD3 and CD69 (Pharmingen) labeled with phycoerythrin were used. Stained cells were processed on a FACScan (Becton Dickinson, Franklin Lakes, NJ). For the analysis of GFP fluorescence standard FITC filter settings were used. FACS data were analyzed with Cell Quest computer software (Becton Dickinson).

Cytokine Production Assay

IL-2 production was measured after 24-hour incubation of Jurkat cells at a concentration of 1×10^6 cells/ml in the absence and presence of PMA, ionomycin, or CD3 and CD3/CD28 antibodies using ELISA kit DuoSet (R&D Systems, Minneapolis, MN) following the manufacturer's protocols. The cytokine production experiments were performed three times, all determinations were done in triplicates.

Radiotracer Assay for TKGFP Expression In Vitro

2′-Fluoro-2′-deoxy-1-β-D-arabinofuranosyl-5-iodouracil (FIAU) accumulation assays were performed to assess the level of TKGFP enzymatic activity in stimulated and nonstimulated wild-type and transduced Jurkat clones, as previously described [12]. Briefly, cells were seeded into six-well tissue culture plates (Falcon, Becton Dickinson) precoated with anti–human CD3 antibody 1 μg/ml (Pharmingen) at a concentration of 3×10^6 cells/well. After 24 hours of stimulation, the incubation medium was replaced with 3 ml of medium containing [2-^{14}C]FIAU 0.01 μCi/ml (56 mCi/mmol) and [*met*-^{3}H]TdR 0.2 μCi/ml (60 Ci/mmol) (Moravek Biochemicals, Brea, CA). The rest of the experimental protocol was conducted as previously described [12]. The ratio of K_i values (the FIAU/TdR ratio) is a measure of *HSV1-tk* activity and correlates with other independent measures of the gene expression [12].

Subcutaneous Infiltrates, Study Groups, and TCR Stimulation In Vivo

The experimental protocol involving animals was approved by the Institutional Animal Care and Use Committee of the Memorial Sloan Kettering Cancer Center. Jurkat cells (5×10^6 cells of each type) in 100 μl of Matrigel (Collaborative Biochemical Products, Bedford, MA) were

injected subcutaneously (s.c.) into 20 *nu/nu* mice (Harlan Sprague–Dawley, Indianapolis, IN) weighing 20 to 25 g. Jurkat cell infiltrates were palpable within 2 weeks and reached a diameter of about 5 mm in 4 weeks post s.c. injection.

TCR-mediated activation of the s.c. Jurkat infiltrates was achieved by IV administration of a purified anti–human CD3 antibody (Antibody Core Facility, Memorial Sloan Kettering Cancer Center) 250 μg/mouse and anti–human CD28 antibody (Pharmingen) 50 μg/mouse twice, at 24 and 6 hours before [^{124}I]FIAU injection. The anti–mouse Ly5.1 antibody (Antibody Core Facility) was used as a negative control.

Assessment of TKGFP Fluorescence In Vivo

Whole-body imaging of TKGFP fluorescence in mice was performed using a home-built digital OFI system consisting of a 150-W halogen light source LT-9500 (Lightools

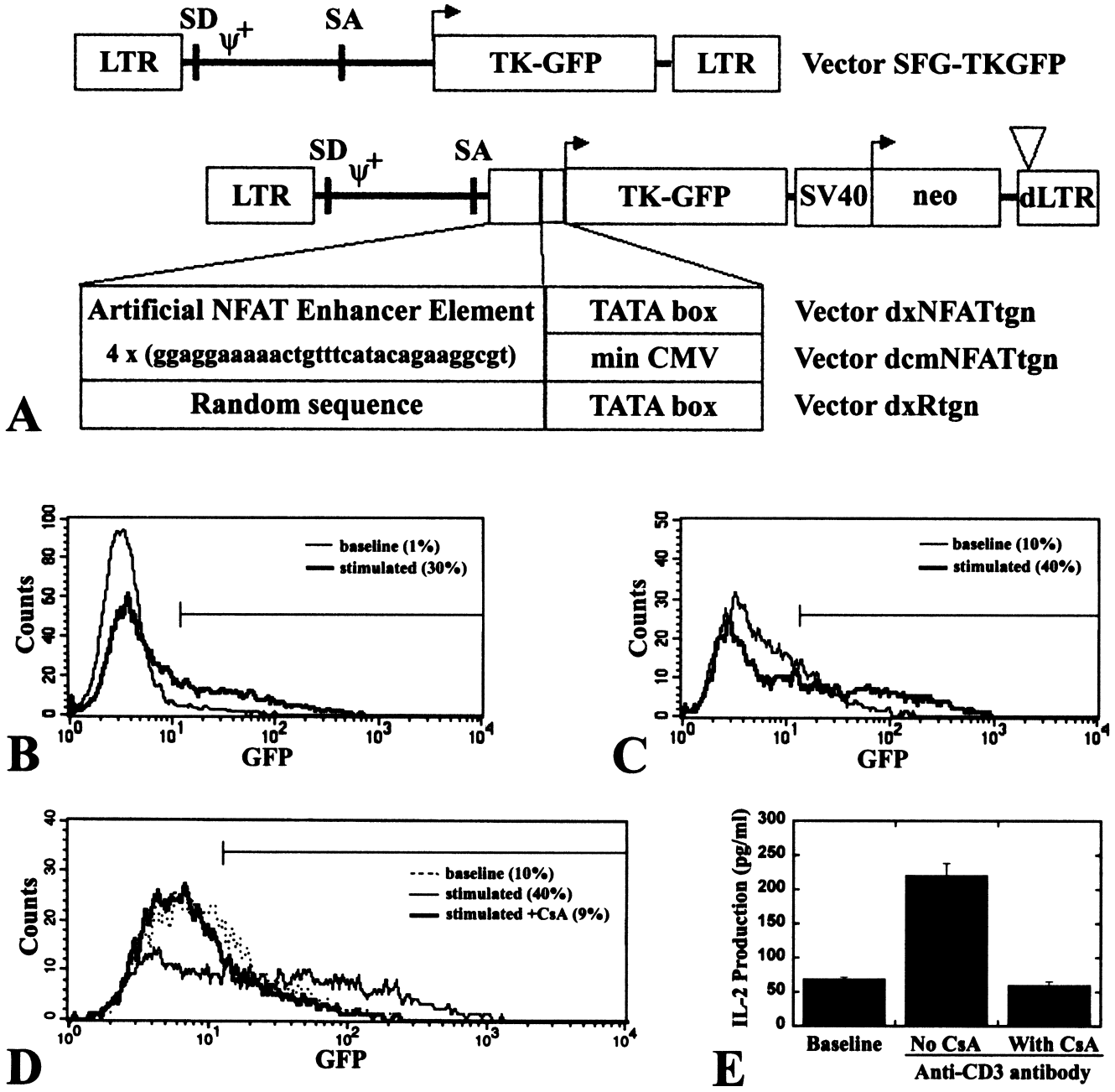

Figure 1. *Schematic structures and functional properties of the NFAT-TKGFP reporter systems. In SFG-TKGFP, the constitutive expression of the TKGFP reporter gene is driven by the retroviral LTR. Expression of the TKGFP reporter gene is driven by four tandem repeats of the NFAT-specific DNA binding motif linked to the minimal E1B promoter in dxNFATtgn, or linked to the minimal CMV promoter in the dcmNFATtgn vector (A). FACS profiles of TKGFP reporter gene expression (TKGFP fluorescence) under nonstimulated basal conditions (thin line) and after stimulation with anti-CD3 antibody (bold line) in mixed populations of Jurkat/dxNFATtgn (B) and dcmNFATtgn (C) cells. The basal and stimulated mean fluorescence in Jurkat/dxNFATtgn cells was 30.2 and 71.8, respectively; in dcmNFATtgn cells the values were 31.4 and 117.4, respectively; the percentage of gated (M1-GFP positive) cells is indicated in parentheses. FACS profiles of TKGFP expression (D) and ELISA measures of IL-2 expression (E) in Jurkat/dcmNFATtgn cells under nonstimulated basal conditions, after stimulation with anti-CD3 antibody, and after stimulation with anti-CD3 antibody in the presence of Cyclosporin A.*

Research, Encinitas, CA) equipped with an excitation filter (480 to 490 nm); two fiberoptic guides with linear illuminators (each positioned at 45°); and an emission filter plate (505-nm cut-off filter; 6×12 cm). The TKGFP fluorescence was easily observed with naked eye and the images were captured using a CCD camera C4742-95-12NR (Hamamatsu, Bridgewater, NJ) attached to a PC running the MCID software (Imaging Research, St. Catharines, Ontario, Canada).

PET Imaging with [^{124}I]FIAU

^{124}I production and [^{124}I]FIAU synthesis was conducted as described by us previously [1]. One day before [^{124}I]FIAU administration, the animals received a 2-ml intraperitoneal (i.p.) injection of a 0.9% NaI solution to block the thyroid uptake of radioactive iodide (small amounts of contaminant). [^{124}I]FIAU was administered IV 300 μCi/animal. PET imaging was performed on an advance PET tomograph (General Electric, Milwaukee, WI) 24 hours after tracer administration to allow for sufficient clearance of body background radioactivity. The 24-hour biologic clearance improved signal-to-noise and specificity of the images.

Animals were anesthetized by i.p. injection of ketamine (87 mg/kg) and xylazine (13 mg/kg). Transmission and emission scans were obtained in 2D mode; the emission scans were corrected for random counts, dead time, and attenuation. The duration of the transmission and emission scans was 15 and 45 minutes, respectively. Images were reconstructed using the iterative reconstruction algorithm [13] yielding slice thickness of 4.2 mm and a transaxial resolution element size of 4 mm^2. Radioactivity concentration in tumors (% dose/g) was measured from the PET images as previously described [1].

To estimate tumor dosimetry of [^{124}I]FIAU and to confirm the PET radioactivity measurements, the individual tumors, muscle, and venous blood were sampled, weighed, and assayed for ^{124}I radioactivity using a Packard 5500 gamma spectrometer (Packard, Meriden, CT). A portion of each infiltrate sample was also used for the assessment of TKGFP and CD69 expression using FACS.

Statistics

Descriptive statistics of group data were performed using univariate analysis. Group data were compared using ANOVA analysis, regression analysis, and Student *t* test; a *P* value of <0.05 was considered significant. Statistical analysis of data was performed using the StatView 4.57 (Abacus Concepts, Cary, NC).

Results

Assessment of NFAT-TKGFP Reporter System in Transduced Jurkat Cells

To assess the NFAT-TKGFP reporter system we developed two self-inactivating retroviral vectors in which the *TKGFP* reporter gene was placed under control of two different artificial NFAT-specific promoters (Figure 1*A*). These promoters contain four NFAT-specific binding site repeats followed by either the E1b minimal promoter (dxNFATtgn vector) or the CMV minimal promoter (dcmNFATtgn vector). Jurkat cells transduced with these vectors were termed Jurkat/dxNFATtgn and Jurkat/dcmNFATtgn, respectively. Jurkat cells transduced with the SFG-TKGFP and dxRtgn vectors were termed Jurkat/TKGFP (positive control) and Jurkat/Rtgn (negative control), respectively.

The level of the *TKGFP* expression in a mixed population of nonstimulated Jurkat/dxNFATtgn cells was similar to that in wild-type Jurkat cells. Twenty-four hours after stimulation with either PMA/ionomycin or anti-CD3 antibody, only approximately 30% of the Jurkat/dxNFATtgn mixed-cell population expressed TKGFP at high levels (Figure 1*B*). Significantly higher levels of *TKGFP* expression after stimulation were achieved in a mixed population of Jurkat/dcmNFATtgn cells, although there was no significant change in the percentage of reactive cells (Figure 1*C*). There was no induction of *TKGFP* expression in Jurkat/Rtgn cells after stimulation (data not shown).

IL-2 production in mixed populations of both Jurkat/dxNFATtgn and Jurkat/dcmNFATtgn cells was equally low

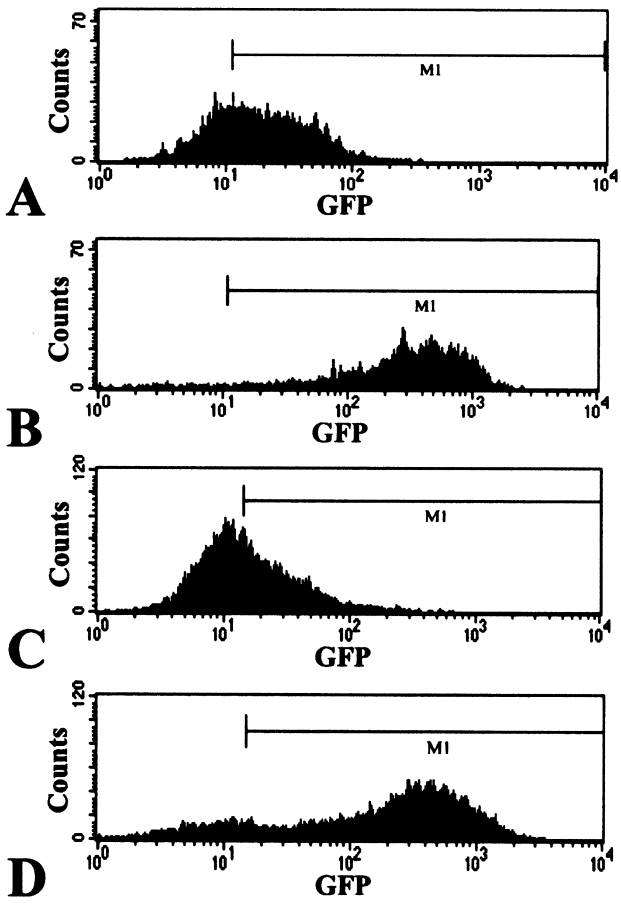

Figure 2. *NFAT-TKGFP reporter system in dcmNFATtgn clones 3 and 4. FACS profiles of TKGFP reporter gene expression under nonstimulated basal conditions and after stimulation with anti-CD3/CD28 antibodies in clones 3 and 4 of Jurkat/dcmNFATtgn cells. The basal and stimulated mean fluorescence in clone 3 was 22.9 (A) and 351.1 (B), respectively, and in clone 4, 25.5 (C) and 419.1 (D), respectively.*

before stimulation and high after stimulation (Figure 1*E*). The specificity of NFAT-mediated *TKGFP* and IL-2 expression was demonstrated by complete inhibition of stimulation by Cyclosporin A (Figure 1*D* and *E*).

Jurkat/dcmNFATtgn mixed-population cells were used further for clonal selection because of higher inducible levels of the *TKGFP*. Two single cell–derived clones (3 and 4) of Jurkat/dcmNFATtgn cells with low background and high inducible levels of *TKGFP* expression were obtained (Figure 2). The dynamics of the dcmNFATtgn reporter system response was studied at different times (24, 48, and 72 hours) following stimulation with anti-CD3 alone, or in combination with anti-CD28 antibodies (Figure 3*A*). The levels of TKGFP, CD69, and IL-2 expression in Jurkat/dcmNFATtgn clones were maximal at 24 hours. The level of *TKGFP* expression gradually decreased over 72 hours of continuous stimulation (in clone 4 more than clone 3), whereas the level of CD69 expression remained high. Insignificant differences in the magnitude of *TKGFP* and CD69 expression in Jurkat/dcmNFATtgn clones were observed during the 24- to 72-hour period of stimulation with anti-CD3 alone or in combination with anti-CD28 antibodies. In contrast, significantly higher levels of IL-2 expression were observed after stimulation with the combination of anti-CD3 and anti-CD28 antibodies, compared with stimulation by anti-CD3 alone (Figure 3*B*). There were no detectable levels of TKGFP, CD69 and IL-2 expression after stimulation with anti-CD28 antibody alone (data not shown).

The level of *TKGFP* expression (HSV1-tk subunit enzymatic activity) in nonstimulated and stimulated Jurkat/dcmNFATtgn clones 3 and 4 was additionally assessed

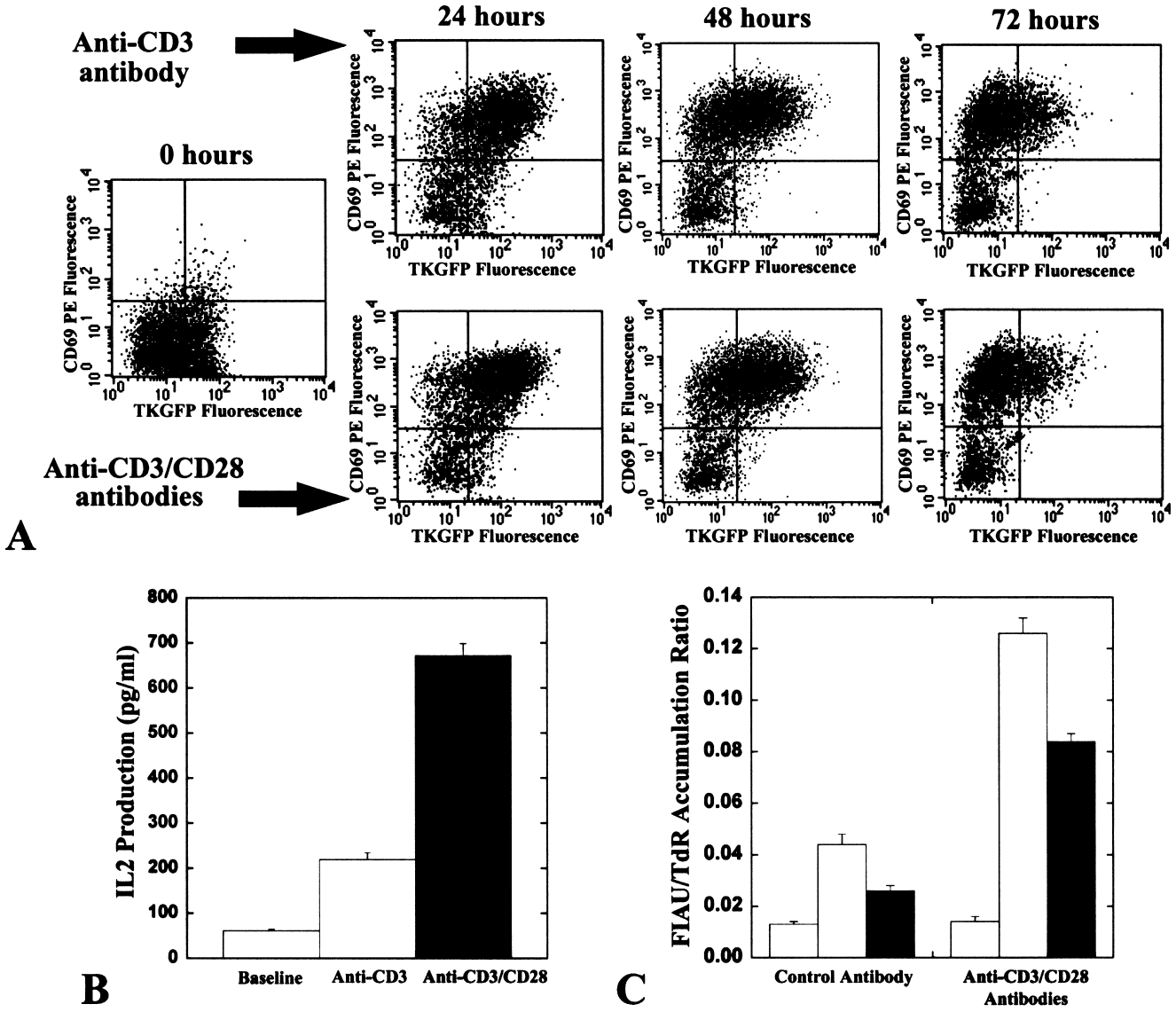

Figure 3. *The dynamics of the dcmNFATtgn reporter system response. The FACS profiles of TKGFP reporter gene and CD69 expression in Jurkat/dcmNFATtgn cells clone 4 under nonstimulated basal conditions and after continuous stimulation with anti-CD3 alone or in combination with anti-CD28 antibodies. The percentage of gated cells in each quadrant is indicated (A). IL-2 production under nonstimulated basal conditions, and after 24-hour stimulation with anti-CD3 alone or in combination with anti-CD28 (B). The radiotracer FIAU/TdR accumulation ratio before and after stimulation with anti-CD3/CD28 antibodies in Jurkat/wild type (blank), Jurkat/dcmNFATtgn clone 3 (shaded), clone 4 (solid) (C).*

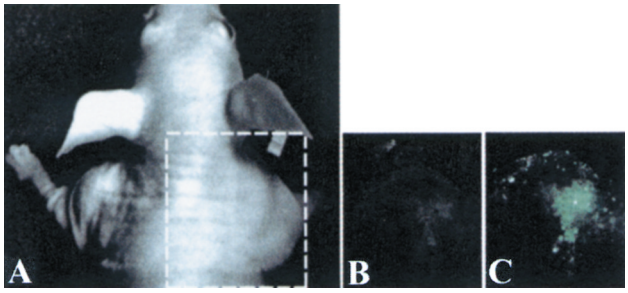

Figure 4. *Optical fluorescence imaging of the NFAT-TKGFP reporter system activity in vivo. Images of TKGFP fluorescence in an s.c. Jurkat/dcmNFATtgn (clone 4) infiltrate were obtained in the same animal (A) before (B) and after treatment (C) with anti-CD3/CD28 antibodies.*

using a radiotracer assay. The increased levels of *TKGFP* expression measured by FACS corresponded with significantly higher levels of [^{14}C]FIAU accumulation in stimulated Jurkat/dcmNFATtgn cells, compared with those in non-stimulated cells (Figure 3*C*). Wild-type Jurkat cells exhibited only insignificant background levels of [^{14}C]FIAU accumulation.

OFI and PET Imaging of the TKGFP Expression in Jurkat Cell Infiltrates After CD3 Stimulation In Vivo

The efficacy of the dcmNFATtgn reporter system *in vivo* was assessed using OFI and PET. Nude mice bearing four s.c. infiltrates were studied: Jurkat/dcmNFATtgn clones 3 and 4, Jurkat/TKGFP (positive control), and wild-type Jurkat (negative control). Half of the animals (n=10) were injected IV with anti-CD3 (500 μg) and anti-CD28 (100 μg) antibodies to induce the NFAT pathway in Jurkat/TKGFP infiltrates; the other half were injected with Ly5.1 control antibody. All animals were injected IV with [^{124}I]FIAU 24 hours after administration of the antibodies, and imaged 24 hours later with OFI and PET.

OFI images of *TKGFP* expression obtained in mice before and after treatment with the control antibody showed no TKGFP fluorescence in both the Jurkat/dcmNFATtgn and wild-type Jurkat infiltrates (Figure 4*A*). In animals treated with the anti-CD3 and anti-CD28 antibodies, a significant increase of TKGFP fluorescence was observed in Jurkat/dcmNFATtgn infiltrates (Figure 4*B*). In contrast no TKGFP fluorescence was observed in wild-type Jurkat infiltrates.

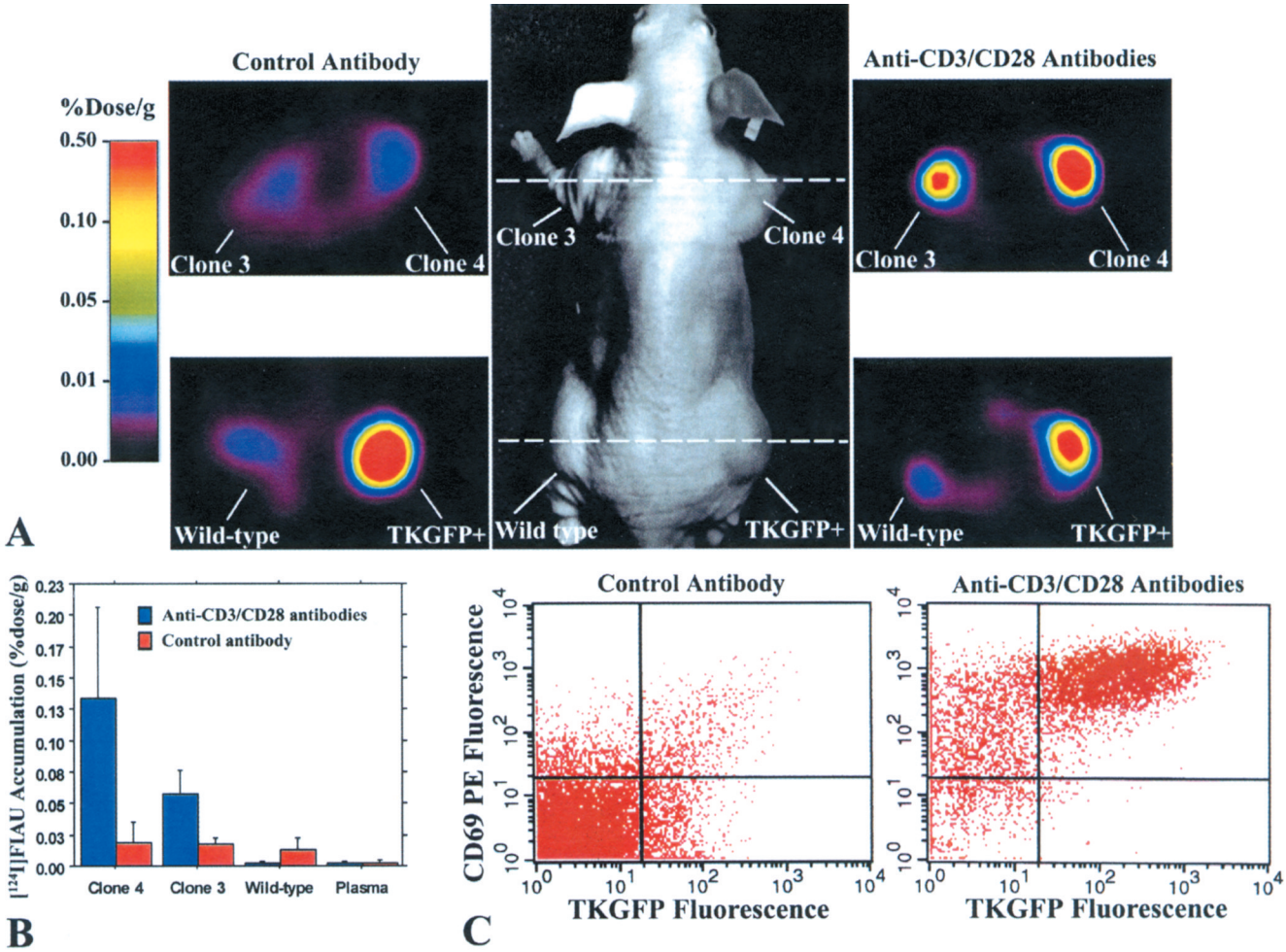

Figure 5. *Imaging NFAT-TKGFP reporter system activity with [^{124}I]FIAU and PET and assessments in tissue samples. Photographic image of a typical mouse bearing different s.c. infiltrates (middle panel); transaxial PET images of TKGFP expression in a mouse treated with control antibody (left panel) and anti-CD3/CD28 antibodies (right panel) were obtained at the levels indicated by the dashed lines (A). [^{124}I]FIAU accumulation (% dose/g) in tissue samples of the Jurkat/dcmNFATtgn clone 3 and 4 infiltrates, wild-type Jurkat infiltrates, and blood plasma, obtained after PET imaging (B). FACS profiles of TKGFP and CD69 expression in a tissue sample from the same Jurkat/dcmNFATtgn clone 4 infiltrate that was imaged with PET (C).*

PET images of [^{124}I]FIAU accumulation obtained in mice treated with control antibody revealed background levels of accumulation of [^{124}I]FIAU in both the Jurkat/dcmNFATtgn and wild-type Jurkat infiltrates (Figure 5*A*). In animals treated with anti-CD3 and anti-CD28 antibodies, a significantly higher accumulation of [^{124}I]FIAU was observed in the Jurkat/dcmNFATtgn infiltrates. The level of radioactivity in activated Jurkat/dcmNFATtgn infiltrates was comparable to that in the constitutively expressing Jurkat/TKGFP infiltrates (positive control) (Figure 5*B*).

FACS analysis of the Jurkat/dcmNFATtgn infiltrates obtained from the Ly5.1 treated animals (noninduced) animals (the same animals that were imaged with OFI and PET) demonstrated base levels of TKGFP and CD69 expression (Figure 5*C*). Similar results were obtained with the wild-type Jurkat infiltrates (data not shown). In contrast, the Jurkat/dcmNFATtgn infiltrates from the animals that were treated with anti-CD3 and anti-CD28 antibodies had a very large fraction (>60%) of cells overexpressing both TKGFP and CD69.

Discussion

The goal of this study was to develop and validate a method for monitoring the activation and location of T lymphocytes *in vivo* using noninvasive imaging techniques. For this purpose, we generated a TKGFP reporter system that specifically responds to TCR activation. We constructed and tested two self-inactivating retroviral vectors bearing an artificial NFAT-sensitive promoter that controls the expression of the *TKGFP* reporter gene. These vectors were used to establish stably transduced mixed and clonal populations of Jurkat cells bearing a functional TCR that are frequently used as a model for T-cell activation [14]. A similar approach using analogous NFAT-sensitive artificial promoter and GFP reporter gene was recently described by others [15]. However, we were not satisfied with inducible levels of the reporter gene expression that were achievable using the promoter construct described in the latter study. During the optimization of our NFAT-sensitive reporter system, we found that the addition of a minimal CMV promoter downstream of four tandem repeats of the NFAT-specific DNA binding sequences (dcmNFATtgn vector) resulted in significantly higher inducible levels of the reporter gene expression and only an insignificant increase in background activity.

The versatility of the *TKGFP* reporter gene allowed for assessment of the NFAT-sensitive reporter system activity by fluorescent microscopy and quantitation by FACS analysis, as well as radiotracer assay [10,12] and PET imaging [1]. FACS allowed for the selection of clones of transduced Jurkat cells with optimal functional characteristics (low background and high inducible activity).

We demonstrated that the *cis*-NFAT-TKGFP reporter system was sufficiently sensitive to image TCR-mediated anti-CD3 antibody stimulation and correlated with the expression of two independent markers of T-cell activation, CD69 and IL-2. The specificity of NFAT-TKGFP reporter system for TCR-mediated T-cell activation was demonstrated by the absence of an increase in *TKGFP* expression in response to the addition of anti-CD28 along with anti-CD3 antibody stimulation, and no *TKGFP* expression in response to anti-CD28 antibody stimulation alone. Importantly, the presence of a functional CD28 costimulatory pathway in transduced cells was demonstrated by the levels of IL-2 expression obtained in response to the combination of anti-CD3 and anti-CD28 antibody stimulation, compared to anti-CD3 alone. As expected, there was no detectable increase in IL-2 expression in response to anti-CD28 stimulation alone. Other studies have demonstrated similar results in Jurkat and primary T cells using a luciferase (Luc)- or GFP-based reporter system and different stimuli to monitor NFAT activation [15–17].

The specificity of our NFAT reporter system was further confirmed by using Cyclosporin A, which is a commonly used immunosuppressive drug that acts through inhibiting calcineurin-mediated dephosphorylation of NFAT [7]. Cyclosporin A completely inhibited the CD3- and CD28-mediated activation of the NFAT-TKGFP reporter system, which further demonstrates the specificity of the NFAT reporter system. These results are in agreement with previously published data using a Luc-reporter system, where the Luc-reporter gene was placed under control of the IL-2 promoter [17]. The inhibitory effects of Cyclosporin A on TCR-dependent activation was demonstrated using the IL-2–Luc system in AAV-transduced Jurkat cells.

A tendency for temporal dissociation in the expression of TKGFP and CD69 markers for TCR-dependent activation was observed. Namely, *TKGFP* expression showed a tendency to decrease beyond 24 hours of continuous stimulation *in vitro*, whereas CD69 expression persisted at the same level during the 24- to 72-hour period. This observation may be explained in part by a decrease of NFAT transcriptional activity as a result of the apoptosis occurring in stimulated Jurkat cells [18]. The duration of NFAT-mediated transcriptional activity may actually be even shorter because the half-life of GFP subunit of TKGFP protein is about 16 hours [19] and may be shorter than that of CD69. To further explore this observation, a short-lived variant of TKGFP reporter protein could be developed using a similar approach that was previously described for GFP [19].

An advantage of the TKGFP dual reporter system is that both fluorescence and nuclear imaging studies can be performed on the same animal [10]. Whole-body OFI demonstrating GFP expression has been described in live mice with s.c. xenografts [20], in studies of metastatic tumor spread [21], neoangiogenesis [22], and transgenic animals [5]. We have extended OFI to visualize the NFAT-TKGFP reporter system in transduced Jurkat s.c. infiltrates. We demonstrated that OFI can be used to visualize the substantial increase of *TKGFP* expression in s.c. Jurkat NFAT-TKGFP infiltrates after stimulation *in vivo*. OFI may provide the means for repetitive noninvasive, semiquantitative temporal monitoring of T-cell activity at superficial locations (subcutaneous, submucosal, pleural, peritoneal, etc.).

PET imaging obviates the current limitations of OFI to imaging superficial lesions. In this report, we have demonstrated that PET is sufficiently sensitive for visualization of *TKGFP* expression (HSV1-tk–derived enzymatic activity) in NFAT-TKGFP–transduced Jurkat infiltrates. We have shown that [^{124}I]FIAU and PET imaging can provide spatial and quantitative information about the process and magnitude of TCR-mediated T-cell activation using the NFAT-TKGFP reporter system. Moreover, the induction of *TKGFP* expression correlated with other independent markers of T-cell activation (e.g., CD69), and was confirmed by direct analysis of tissue samples. These combined *in vitro* and *in vivo* results demonstrate that the images of NFAT-TKGFP reporter system activity obtained with [^{124}I]FIAU and PET reflect the status of the TCR-dependent NFAT-mediated signaling pathway.

Although PET imaging 24 hours after radiotracer administration is not well suited for T-cell trafficking and activation studies, recent reports [23,24] and results from our laboratory [25] show that FIAU imaging can be performed as soon as 10 to 30 minutes after tracer administration. Radiolabeling of FIAU with ^{18}F (110 minutes half-life) or ^{11}C (20 minutes half-life) is feasible [26,27] and would provide the opportunity for repetitive imaging studies.

PET imaging of T-lymphocytic activation using the NFAT-TKGFP reporter system could potentially be used to assess efficacy and optimize T-cell doses in immunotherapies. For example, in CTL-based therapies (antitumor, antiviral, etc.), T cells obtained from a patient could be transduced with the NFAT-TKGFP reporter system, sensitized against certain antigens, and administered back to the patient. PET imaging could be performed to visualize the sites of transduced CTL activation and targeting. Also, it could be feasible to use the NFAT-TKGFP reporter system and PET imaging for the assessment of new immunotherapeutic approaches, including dendritic cell, DNA, RNA and peptide vaccines, or new immunosuppressive therapies. It may also find applications in monitoring T-cell involvement in graft-versus-host-disease after bone marrow transplantation and during the process of organ transplant rejection.

In summary, we have demonstrated for the first time that noninvasive OFI and nuclear imaging of T-cell activation is feasible using the NFAT-TKGFP reporter system. We have demonstrated that PET imaging with [^{124}I]FIAU using the NFAT-TKGFP reporter system is sufficiently sensitive to detect transcriptional upregulation in the TCR-dependent NFAT-mediated signal transduction pathway. PET imaging of TCR-induced NFAT transcriptional activity may be useful in the assessment of T-cell responses and immunotherapy.

References

[1] Tjuvajev JG, Avril N, Oku T, Sasajima T, Miyagawa T, Joshi R, Safer M, Beattie B, DiResta G, Daghighian F, Augensen F, Koutcher J, Zweit J, Humm J, Larson SM, Finn R, and Blasberg R (1998). Imaging herpes virus thymidine kinase gene transfer and expression by positron emission tomography. *Cancer Res* **58**, 4333–4341.

[2] Blasberg RG, and Tjuvajev JG (1999). Herpes simplex virus thymidine kinase as a marker/reporter gene for PET imaging of gene therapy. *Q J Nucl Med* **43**, 163–169.

[3] Gambhir SS, Herschman HR, Cherry SR, Barrio JR, Satyamurthy N, Toyokuni T, Phelps ME, Larson SM, Balatoni J, Finn R, Sadelain M, Tjuvajev J, and Blasberg R (2000). Imaging transgene expression with radionuclide imaging technologies. *Neoplasia* **2**, 118–138.

[4] Jacobs A, Tjuvajev JG, Dubrovin M, Akhurst T, Balatoni J, Beattie B, Joshi R, Finn R, Larson SM, Herrlinger U, Pechan PA, Chiocca EA, Breakefield XO, and Blasberg RG (2001). Positron emission tomography-based imaging of transgene expression mediated by replication-conditional, oncolytic herpes simplex virus type 1 mutant vectors *in vivo*. *Cancer Res* **61**, 2983–2995.

[5] Yang M, Baranov E, Moossa AR, Penman S, and Hoffman RM (2000). Visualizing gene expression by whole-body fluorescence imaging. *Proc Natl Acad Sci USA* **97**, 12278–12282.

[6] Kiani A, Rao A, and Aramburu J (2000). Manipulating immune responses with immunosuppressive agents that target NFAT. *Immunity* **12**, 359–372.

[7] Crabtree GR (1999). Generic signals and specific outcomes: signaling through Ca*2+*, calcineurin, and NF-AT. *Cell* **96**, 611–614.

[8] Rao A, Luo C, and Hogan PG (1997). Transcription factors of the NFAT family: regulation and function. *Annu Rev Immunol* **15**, 707–747.

[9] Aramburu J, Rao A, and Klee CB (2000). Calcineurin: from structure to function. *Curr Top Cell Regul* **36**, 237–295.

[10] Jacobs A, Dubrovin M, Hewett J, Sena-Esteves M, Tan CW, Slack M, Sadelain M, Breakefield XO, and Tjuvajev JG (1999). Functional coexpression of HSV-1 thymidine kinase and green fluorescent protein: implications for noninvasive imaging of transgene expression. *Neoplasia* **1**, 154–161.

[11] Riviere I, and Sadelain M (1997). *Gene Therapy Protocols: Methods in Molecular Biology*. Humana Press, Totowa, NJ, pp. 59–78.

[12] Tjuvajev JG, Stockhammer G, Desai R, Uehara H, Watanabe K, Gansbacher B, and Blasberg RG (1995). Imaging the expression of transfected genes *in vivo*. *Cancer Res* **55**, 6126–6132.

[13] Tjuvajev JG, Joshi A, Callegari J, Lindsley L, Joshi R, Balatoni J, Finn R, Larson SM, Sadelain M, and Blasberg RG (1999). A general approach to the non-invasive imaging of transgenes using *cis*-linked herpes simplex virus thymidine kinase. *Neoplasia* **1**, 315–320.

[14] Li W, and Handschumacher RE (1996). Regulation of the nuclear factor of activated T cells in stably transfected Jurkat cell clones. *Biochem Biophys Res Commun* **219**, 96–99.

[15] Hooijberg E, Bakker AQ, Ruizendaal JJ, and Spits H (2000). NFAT-controlled expression of GFP permits visualization and isolation of antigen-stimulated primary human T cells. *Blood* **96**, 459–466.

[16] Shapiro VS, Mollenauer MN, and Weiss A (1998). Nuclear factor of activated T cells and AP-1 are insufficient for IL-2 promoter activation: requirement for CD28 up-regulation of RE/AP. *J Immunol* **161**, 6455–6458.

[17] Zhang PX, and Fuleihan RL (1999). Transfer of activation-dependent gene expression into T cell lines by recombinant adeno-associated virus. *Gene Ther* **6**, 182–189.

[18] Su X, Cheng J, Liu W, Liu C, Wang Z, Yang P, Zhou T, and Mountz JD (1998). Autocrine and paracrine apoptosis are mediated by differential regulation of Fas ligand activity in two distinct Jurkat T cell populations. *J Immunol* **160**(11), 5288–5293.

[19] Corish P, and Tyler-Smith C (1999). Attenuation of green fluorescent protein half-life in mammalian cells. *Protein Eng* **12**, 1035–1040.

[20] Lai CC, Gouras P, Doi K, Tsang SH, Goff SP, and Ashton P (2000). Local immunosuppression prolongs survival of RPE xenografts labeled by retroviral gene transfer. *Invest Ophthalmol Vis Sci* **41**, 3134–3141.

[21] Jung S, Ackerley C, Ivanchuk S, Mondal S, Becker LE, Rutka JT (2001). Tracking the invasiveness of human astrocytoma cells by using green fluorescent protein in an organotypical brain slice model. *J Neurosurg* **94**, 80–89.

[22] Fukumura D, Xavier R, Sugiura T, Chen Y, Park EC, Lu N, Selig M, Nielsen G, Taksir T, Jain RK, and Seed B (1998). Tumor induction of VEGF promoter activity in stromal cells. *Cell* **94**, 715–725.

[23] Haubner R, Avril N, Hantzopoulos PA, Gansbacher B, and Schwaiger M (2000). *In vivo* imaging of herpes simplex virus type 1 thymidine kinase gene expression: early kinetics of radiolabelled FIAU. *Eur J Nucl Med* **27**, 283–291.

[24] Brust P, Haubner R, Friedrich A, Scheunemann M, Anton M, Koufaki ON, Hauses M, Noll S, Noll B, Haberkorn U, Schackert G, Schackert H, Avril N, and Johannsen B (2001). Comparison of [^{18}F]FHPG and [$^{124/125}$I]FIAU for imaging herpes simplex virus type 1 thymidine kinase gene expression. *Eur J Nucl Med* **28**, 721–729.

[25] Gelovani Tjuvajev J, Doubrovin M, Akhurst T, Cai S, Balatoni J, Alauddin MM, Finn R, Beattie B, Conti P, and Blasberg RG (2001). Comparison of radiolabeled nucleoside probes (FIAU, FHBG and FHPG) for PET imaging of HSV1-tk gene expression. *J Nucl Med* (in press).

[26] Collins JM, Klecker RW, and Katki AG (1999). Suicide prodrugs activated by thymidylate synthase: rationale for treatment and noninvasive imaging of tumors with deoxyuridine analogues. *Clin Cancer Res* **5**, 1976–1981.

[27] Vander Borght T, Labar D, Pauwels S, and Lambotte L (1991). Production of [2-^{11}C]thymidine for quantification of cellular proliferation with PET. *Int J Radiat Appl Instrum* **42**, 103–104.